Communication: Many-body stabilization of non-covalent interactions: Structure, stability, and mechanics of $Ag_3Co(CN)_6$ framework

Xiaofei Liu, Jan Hermann, and Alexandre Tkatchenko

Citation: J. Chem. Phys. **145**, 241101 (2016); doi: 10.1063/1.4972810
View online: http://dx.doi.org/10.1063/1.4972810
View Table of Contents: http://aip.scitation.org/toc/jcp/145/24
Published by the American Institute of Physics

Communication: Many-body stabilization of non-covalent interactions: Structure, stability, and mechanics of $Ag_3Co(CN)_6$ framework

Xiaofei Liu,[1,2] Jan Hermann,[1] and Alexandre Tkatchenko[1,3]
[1]*Fritz-Haber-Institut der Max-Planck-Gesellschaft, Faradayweg 4-6, D-14195 Berlin, Germany*
[2]*State Key Laboratory of Mechanics and Control of Mechanical Structures, Key Laboratory for Intelligent Nano Materials and Devices of Ministry of Education, Nanjing University of Aeronautics and Astronautics, Nanjing 210016, China*
[3]*Physics and Materials Science Research Unit, University of Luxembourg, L-1511 Luxembourg*

(Received 28 September 2016; accepted 8 December 2016; published online 22 December 2016)

Stimuli-responsive metal-organic frameworks (MOFs) and other framework materials exhibit a broad variety of useful properties, which mainly stem from an interplay of strong covalent bonds within the organic linkers with presumably weak van der Waals (vdW) interactions which determine the overall packing of the framework constituents. Using $Ag_3Co(CN)_6$ as a fundamental test case—a system with a colossal positive and negative thermal expansion [A. L. Goodwin *et al.*, Science **319**, 794 (2008)]—we demonstrate that its structure, stability, dielectric, vibrational, and mechanical properties are critically influenced by many-body electronic correlation contributions to non-covalent vdW interactions. The $Ag_3Co(CN)_6$ framework is a remarkable molecular crystal, being visibly stabilized, rather than destabilized, by many-body vdW correlations. A detailed comparison with $H_3Co(CN)_6$ highlights the crucial role of strongly polarized metallophilic interactions in dictating the exceptional properties of denser MOFs. Beyond MOFs, our findings indicate that many-body electronic correlations can substantially stabilize polarizable materials, providing a novel mechanism for tuning the properties of nanomaterials with intricate structural motifs. *Published by AIP Publishing.* [http://dx.doi.org/10.1063/1.4972810]

Metal-organic frameworks (MOFs) are versatile compounds consisting of metal ions or clusters coordinated to organic linkers that can adopt a multitude of structures varying in dimensionality and topology. MOFs have been shown to exhibit a broad range of useful properties, which can be utilized in applications to molecular storage, gas separation, catalysis, as well as piezoelastic and optical sensors.[1–6] From a large repertoire of framework architectures, MOFs characterized by "wine-rack" and honeycomb topologies have received particular attention due to their ability to yield unprecedentally large responses to external stimuli such as pressure and temperature.[7,8] Due to the low stiffness and the large internal void space, non-covalent van der Waals (vdW) interactions play a critical role in MOFs, determining the unit-cell structure, anisotropic elastic properties, and relative stabilities between various phases.[9–13] In order to enhance our understanding of the internal stabilization mechanisms of MOFs and to enable the future rational control of their properties and functions, here we present a systematic study of $Ag_3Co(CN)_6$ and its hydrogenated analog $H_3Co(CN)_6$. Although it does not contain any organic component, and hence, strictly speaking, does not qualify as a MOF, it is nevertheless a prime example of a framework material, and as such, has a great relevance for MOFs in general. We will therefore speak of MOFs in the following when meaning MOFs and related structures.

The $Ag_3Co(CN)_6$ crystal has been shown to exhibit a colossal positive and negative thermal expansion,[8] which is reflected by the negative linear compressibility that is an order-of-magnitude larger than that of most other materials.[14] The properties of $Ag_3Co(CN)_6$ have been previously studied using density functional theory (DFT) with semi-local functionals and empirical dispersion corrections, either by adding a *post hoc* Ag···Ag vdW term[12] or by using an empirical DFT−D2 approach of Grimme.[15] While the unit-cell volume of $Ag_3Co(CN)_6$ was reproduced relatively accurately in these studies, we show here that this was a result of a lucky coincidence, rather than the evidence of transferable description. We show in this work that modern and more robust dispersion methods which however do not incorporate full many-body contributions (Grimme's DFT−D3,[16] Tkatchenko-Scheffler DFT+vdW method,[17] as well as the non-local vdW-DF functional[18]) significantly overestimate the unit-cell volume of $Ag_3Co(CN)_6$, and, as a consequence, are unable to correctly predict all other properties of this material. (For simplicity, we will refer to this class of methods as pairwise in the following, even though the D3 method is corrected with a 3-body term.) This is an unexpected finding, since most commonly one would expect many-body dispersion effects to enlarge the unit cell of molecular crystals because of the generally repulsive Axilrod-Teller term. In contrast, due to the peculiar geometry of $Ag_3Co(CN)_6$ (see Fig. 1) and strong polarization induced by argentophilic interactions, many-body vdW correlations increase the stability of $Ag_3Co(CN)_6$, reducing its unit cell volume by more than 10% when compared to pairwise vdW methods.

The DFT calculations in this work were performed with the all-electron full-potential FHI-aims code.[19] The numeric atom-centered orbital *tier1* basis set was used for the expansion of the Kohn-Sham wavefunction and a k-point mesh of

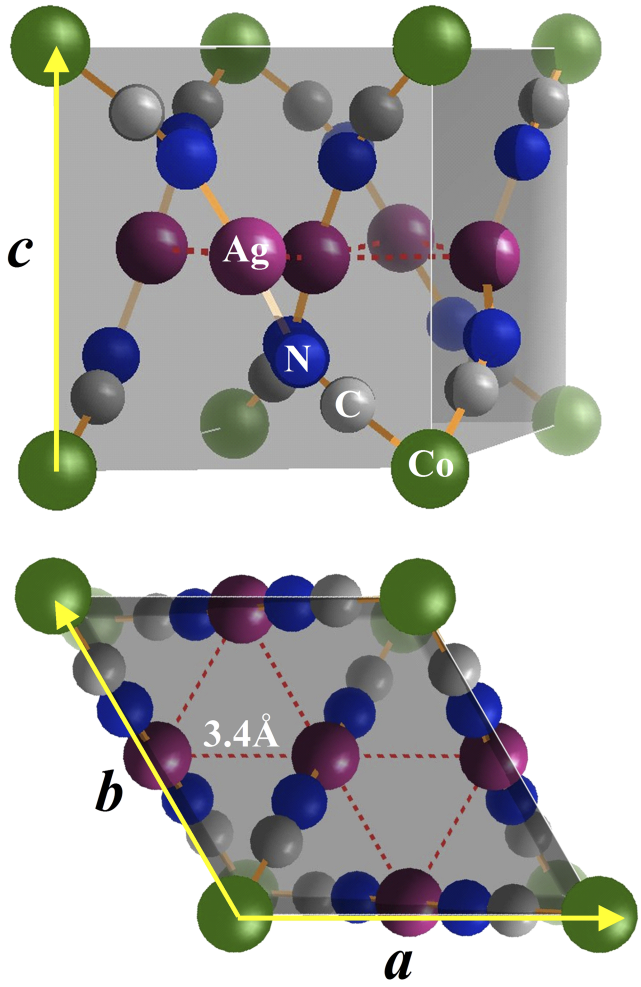

FIG. 1. Side and top views of the $Ag_3Co(CN)_6$ unit cell with Ag atoms in violet, Co in green, N in blue, and C in gray.

$5 \times 5 \times 5$ was adopted for the Brillouin zone sampling. These settings are sufficiently converged, leading to an accuracy of 0.005 Å in interatomic distances and 0.02 eV in absolute lattice energies. The Perdew-Burke-Ernzernhof (PBE) functional[20] was used for the semi-local exchange-correlation energy, and the long-range dispersion interactions were included either by using the Tkatchenko-Scheffler (TS) method[17] or the many-body dispersion method with range-separated self-consistent screening (MBD@rsSCS, referred to as MBD in what follows).[21,22] For completeness, additional calculations have also been carried out with the local-density approximation (LDA), standard PBE functional, PBE with Grimme's D3 dispersion correction (with the 3-body correction),[16] and the non-local vdW-DF functional[18] with revPBE[23] and an optimized exchange.[24] The equilibrium geometries were determined by a full unit cell and internal geometry relaxation with fully analytic forces for PBE and PBE+TS methods and finite-difference forces for the MBD energy. The elastic constants were calculated by a finite-difference method, and the linear compressilibities were obtained from compliance constants, $S_{ij} = \partial\varepsilon_i/\partial\sigma_j$, as $\beta_i = \sum_{j=1}^{3} S_{ij}$. The phonon densities of states were calculated using a $2 \times 2 \times 2$ supercell and a $20 \times 20 \times 20$ Monkhorst-Pack k-grid, using the dynamical matrix computed within the Phonopy code[25] coupled with FHI-aims. Selected results were obtained with the VASP code,[26] in particular for the vdW-DF calculations.

Prior to the analysis of the role of vdW dispersion interactions and many-electron correlations in the properties of $Ag_3Co(CN)_6$, it is instructive to discuss a few notable features of the peculiar structure of this MOF, shown in Fig. 1. The $Ag_3Co(CN)_6$ structure corresponds to a trigonal $P\bar{3}1m$ unit cell. The Ag ions are arranged at the vertices of a two-dimensional Kagome lattice, with the octahedral $[Co(CN)_6]$ ions positioned above and below the silver Kagome hexagons. There are a number of interesting points about interatomic distances in this structure. First, the separation between neighboring Ag ions is ≈3.4 Å, which is rather small, considering the Coulomb repulsion between Ag ions. The closest Co–Co contacts of 6.7 Å are equivalent to the a and b lattice constants ($a = b$ by symmetry). The distance between Ag and Co layers of 3.7 Å is equal to $c/2$. However, the closest Ag–Co contact has a larger value of 5.0 Å, since the Co atoms lie in the middle of Ag hexagons. The Hirshfeld analysis of the electron density yields partial charges of $+0.04|e|$ on Co atoms and $+0.29|e|$ on Ag atoms (nitrogens carry an effective negative charge). Partial charges are quite sensitive to the choice of the partitioning scheme,[27] and it is known that Hirshfeld charges tend to be underestimated, but they should still give the right order of magnitude. Hence, both the triangular Co lattice and Kagome Ag lattice are strongly polarizable, which can lead to non-trivial polarization/dispersion coupling effects that will be reflected in a large contribution of many-body vdW correlations (up to high orders in the perturbation theory) to the properties of $Ag_3Co(CN)_6$. The Co–Co separation is much larger than the Ag–Ag separation in the Kagome lattice; hence the structure and stability of the $Ag_3Co(CN)_6$ framework are determined by a subtle interplay between vdW interactions within and between the Co and Ag sublattices. Namely, the interaction between adjacent Co layers and between the Ag and Co lattices will tend to decrease the c lattice constant, while the in-plane Ag···Ag interactions will lead to the contraction of the a/b lattice constants. However, the strong covalent bonds in the Co–CN–Ag–NC–Co linkages impose the constraint that a contraction in a/b or c lattice constants must be coupled with an expansion in the orthogonal direction(s).

We start by discussing the performance of the standard semi-local DFT approximations in determining the structure of $Ag_3Co(CN)_6$. The potential-energy surface of this system along the a and c lattice directions, as well as the performance of several methods on the unit cell vectors and the unit cell volume are shown in Figs. 2 and 3, respectively. Detailed information about the lattice constants and unit cell volumes calculated with different approaches is available in the supplementary material. Previous works[28] as well as our own calculations show that the LDA significantly overestimates the cohesion in this framework, yielding a unit cell volume that is too small by 14.3% compared to low-temperature (10 K) experiments. The performance of the standard PBE functional is very similar, but instead of an underestimation we observe an overestimation of 15.2% in the unit cell volume. Therefore, neither LDA nor PBE is able to correctly account for the complex set of interactions within the $Ag_3Co(CN)_6$ framework. The inclusion of pairwise dispersion corrections on top of the PBE functional improves

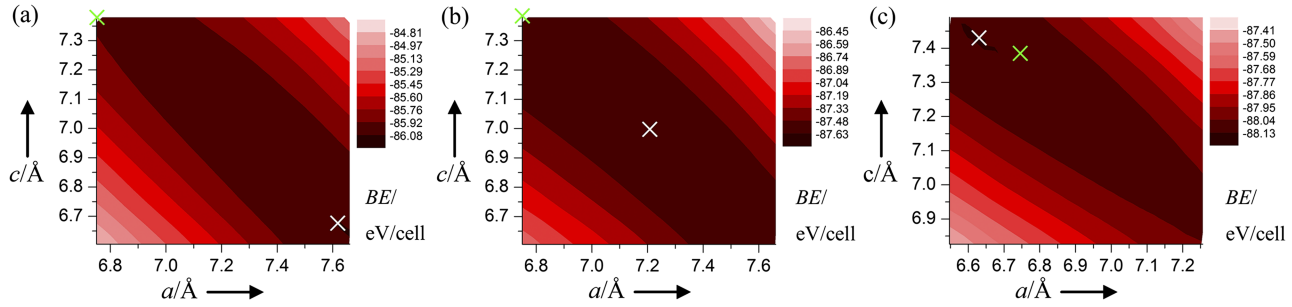

FIG. 2. Potential-energy surface (PES) of $Ag_3Co(CN)_6$ as a function of lattice constants c and a/b, calculated with (a) PBE, (b) PBE+TS, (c) PBE+MBD. The white cross indicates the minimum of the corresponding PES, whereas the green cross indicates the experimental minimum structure. BE stands for binding energy in units of eV/cell. See the supplementary material for the fine-grained energy surface of PBE+MBD around the equilibrium lattice constant.

the situation. Previous work has already shown that using the empirical PBE–D2 method by Grimme leads to a good agreement for the structure of $Ag_3Co(CN)_6$ in comparison to the experiment.[15] This agreement is, however, purely accidental. The empirical D2 approximation disregards coordination, ionicity, and other electronic structure effects on vdW interactions. It also uses a crude definition of vdW parameters for elements beyond the second period. In fact, the use of modern

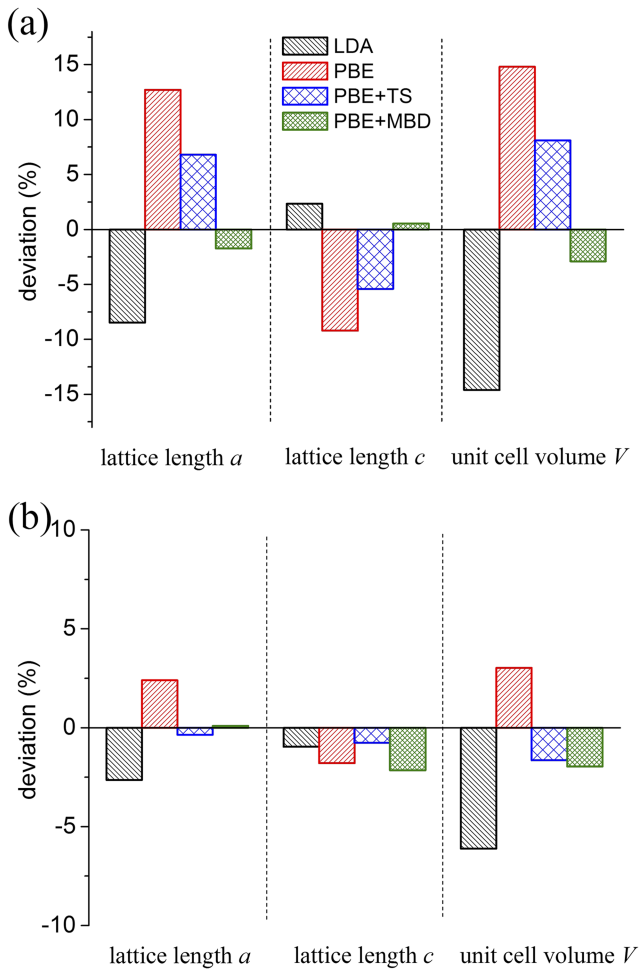

FIG. 3. Deviation of lattice constants a, c and the unit-cell volume V of the equilibrium geometry as calculated with LDA, PBE, PBE+TS, and PBE+MBD methods with respect to the low-temperature experiment for (a) $Ag_3Co(CN)_6$[15] and (b) $H_3Co(CN)_6$.[31] The values of lattice constants are shown in the supplementary material.

and more robust pairwise interatomic vdW approaches, such as PBE–D3 and PBE+TS, demonstrates that these methods perform visibly better than LDA or PBE, yet they still considerably *underestimate* the binding in $Ag_3Co(CN)_6$. PBE–D3 yields a unit-cell volume which is by 4.5% too large, while PBE+TS overestimates the volume by 7.8%. This arises from an error of 0.25 Å in PBE–D3 for the a/b directions vs. an error of 0.46 Å in the case of PBE+TS. The slightly different performance of PBE–D3 can be explained by the fact that the D3 correction disregards any effects beyond the simple coordination dependence, while the TS method does consider the partially ionic nature of the $Ag_3Co(CN)_6$ framework by defining all vdW parameters as functionals of the electron density. For completeness, we also note that the vdW-DF functional[18] also underbinds, leading to errors of 0.38 Å in a/b and 0.1 Å in the c lattice constants. Putting aside the comparison between different pairwise vdW methods, it is evident that these methods are insufficient to provide an accurate description of MOFs with nontrivial dispersion interactions between its metallic and organic components. This is in stark contrast to purely organic molecular crystals (OMCs), where both PBE–D3 and PBE+TS methods are able to achieve a consistent accuracy of 1%–2% in the unit cell volumes.[29,30] In addition, it is noteworthy that both PBE–D3 and PBE+TS *underbind* $Ag_3Co(CN)_6$, whereas an opposite behavior is often observed for OMCs. In OMCs, the inclusion of a repulsive Axilrod-Teller-Muto (ATM) term is found to improve the agreement with experimental structures and lattice energies. In contrast, the inclusion of a repulsive ATM term and vibrational zero-point effects would lead to even larger underbinding in the case of $Ag_3Co(CN)_6$. This suggests that there must be a very different mechanism that controls the structure and stability of MOFs beyond the widely used pairwise approximations for the vdW energy.

In order to understand the role of non-covalent vdW interactions in the different properties of $Ag_3Co(CN)_6$, it is instructive to first consider the electronic structure of this framework. $Ag_3Co(CN)_6$ is an insulator with a gap of 4.7 eV (calculated using the DFT-HSE06 functional). However, the components of the static dielectric tensor $\epsilon = \{3.7, 3.7, 4.2\}$, calculated using the density-functional perturbation theory (DFPT), are significantly larger than one would expect for standard OMCs (ϵ between 2 and 3). The anisotropy of the dielectric tensor is related to the Co and Ag layers and indicates a non-trivial response, which must play a substantial role in the vdW energy. Furthermore, the DFPT calculations

based on semi-local functionals are likely to underestimate the components of the dielectric tensor of MOFs, due to the lack of the self-consistent treatment of vdW interactions, which may polarize the electron density into the interstitial regions,[32] thereby increasing the dielectric response. In fact, experimental measurements on $KMn[Ag(CN)_2]_3$, which is isostructural to $Ag_3Co(CN)_6$, yield a value of $\epsilon_{33} > 5.9$.[33] Remarkably, this value is closer to diamond than it is to OMCs. These non-trivial polarization effects and their coupling to the dispersion energy are treated to all orders in the dipole approximation by the many-body dispersion (MBD) method.[21,22] The non-additive/non-local polarization response in the MBD method arises from many-body kinetic energy contributions between overlapping quantum harmonic oscillators,[34] treated to infinite order in the pertubration theory. This allows the MBD approach to accurately describe the polarizability tensor of molecules and materials, as has been documented for a wide range of systems.[34–36]

The PBE+MBD method is able to accurately capture the complex vdW correlations in $Ag_3Co(CN)_6$ as demonstrated in Figs. 2 and 3. As shown in the supplementary material, PBE+MBD yields an accuracy of 0.11 Å in *a*/*b* and 0.04 Å in the *c* direction. In contrast to pairwise dispersion methods, the unit-cell volume is slightly underestimated by the PBE+MBD calculations, as it should be since the inclusion of zero-point energy will increase the volume. In addition, further reduction of the error can be expected by using a hybrid functional coupled with the MBD energy.[37] It is remarkable that the PBE+MBD lattice energy is larger by 0.5 eV per unit cell than with PBE+TS, further reflecting the large dielectric polarization in the $Ag_3Co(CN)_6$ framework.

To unveil the role of metallophilic interactions in $Ag_3Co(CN)_6$, it is instructive to compare its structure with the $H_3Co(CN)_6$,[31] which has a similar framework structure as $Ag_3Co(CN)_6$. Using experimental lattice constants, the hydrogenated framework has the unit cell reduced by 0.34 Å in the *a*/*b* directions and a more significant 1.66 Å reduction in the *c* direction due to attractive Co–Co interactions. In addition, the measured thermal expansion coefficient is smaller by an order of magnitude.[38] Due to the absence of Ag···Ag vdW correlations, both the standard functionals and their vdW-inclusive counterparts yield good results for the lattice constants of $H_3Co(CN)_6$ (Fig. 3(b)). LDA underestimates both *a*/*b* and *c* in $H_3Co(CN)_6$, which is different from the trend in $Ag_3Co(CN)_6$. The deviations of lattice constants by PBE show the same trend as in $Ag_3Co(CN)_6$ but are not that significant. The inclusion of the vdW energy leads to a slight underestimation of the *c* lattice constant. Once again, the MBD energy is larger than the TS energy, which stems from the increased polarizability of the Co lattice. These results reinforce the importance of Ag···Ag vdW correlations in determining the correct structure and stability of $Ag_3Co(CN)_6$. Based on this comparison, we expect that a similar many-body stabilization could be observed in other framework structures with strongly polarizable components.

As already discussed in the Introduction, MOFs attract special attention due to their remarkable elastic properties. Table I shows the calculated linear compressibilities of $Ag_3Co(CN)_6$ under hydrostatic pressure. PBE+MBD calculations at 0 K result in $\beta_{ab} = 69.6$ TPa^{-1} and $\beta_c = -36.3$ TPa^{-1}, underestimating the experimental compressibilities at 300 K as expected due to the lack of anharmonicities. The deviations of LDA and PBE–D2 are more significant, with errors exceeding 60% compared to experimental results. As the linear compressibilities depend on elastic properties, we also analyzed the stiffness matrix. The non-diagonal element C_{13} is much higher than C_{11} and C_{12}, which reflects the strong mechanical coupling between the *a*/*b* and *c* axes under hydrostatic pressure and complies with the hinging mechanism of negative linear compressibility. The four elastic constants from PBE–D2 and LDA are larger than those from PBE+MBD, especially the C_{11} from PBE–D2 and C_{33} from LDA, rationalizing the larger compressibilities by MBD. In the case of bulk modulus, the PBE+MBD method yields a value closer to the experiment. The bulk modulus decreases with increasing temperature, and fully anharmonic calculations are expected to yield an even better agreement between PBE+MBD and experiments.

TABLE I. The calculated elastic constants (C), compressibilities (β), and bulk modulus (B) for $Ag_3Co(CN)_6$. The experimental, PBE–D2, and LDA results are from Refs. 14, 15, and 28, respectively.

	Expt.$^{300\ K}$	LDA	PBE–D2	PBE+MBD
β_{12} (TPa^{-1})	115(8)	45.2	42.4	69.6
β_3 (TPa^{-1})	−76(9)	−18.9	−21.2	−36.3
B (GPa)	6.5	11.4	15.8	9.7
C_{11} (GPa)	···	28.6	34.3	26.3
C_{33} (GPa)	···	165.2	139.6	133.8
C_{12} (GPa)	···	12.5	13.1	10.1
C_{13} (GPa)	···	45.5	47.1	42.2

The behavior of MOFs at finite temperature is dictated by low-energy vibrations. In Fig. 4, we show the low-energy phonon density-of-states (DOSs) of $Ag_3Co(CN)_6$ calculated with PBE, PBE+TS, and PBE+MBD methods. The pairwise vdW energy at the TS level lowers the frequencies of the first and second in-plane acoustic phonon modes, which mainly correspond to the vibrations of the Ag lattice normal to the Co–CN–Ag–NC–Co linker. Moreover, the three optical phonon modes of the lowest frequencies are red-shifted by the TS method, and the 3rd and 4th optical phonon modes at Γ are inverted in energy compared to PBE

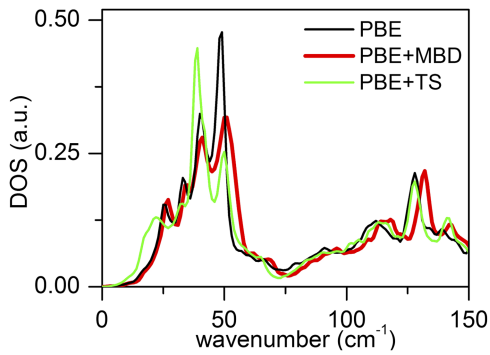

FIG. 4. Phonon density of states for $Ag_3Co(CN)_6$ calculated with PBE, PBE+TS, and PBE+MBD methods. All calculations are done for the optimized PBE+MBD structure.

(see the supplementary material for details). In contrast, the MBD energy increases the frequencies of the 5th and 6th optical phonon modes, leading to a blue shift and broadening of the DOS peak near 50 cm^{-1}. Most surprisingly, many-body effects slightly increase the frequencies of bond stretches, whereas the pairwise TS energy does not exhibit this feature.

In conclusion, we have demonstrated the crucial role of many-body van der Waals correlations (polarization/dispersion coupling) in the structure, stability, dielectric, vibrational, and mechanical properties of metal-organic framework $Ag_3Co(CN)_6$. To our knowledge, $Ag_3Co(CN)_6$ is the first material of its kind where the inclusion of many-body vdW correlations leads to a large contraction of the unit cell and a strong stabilization of the framework. These findings enhance our understanding of the internal stabilization mechanisms of MOFs and provide yet another avenue for controlling the exceptional properties of this class of intricate materials.

See supplementary material for structural details of $Ag_3Co(CN)_6$ and $H_3Co(CN)_6$ calculated with different electronic structure methods, additional calculation details, and phonon data.

A.T. acknowledges support from the European Research Council (ERC Start Grant VDW-CMAT). X.L. is thankful for support from the 973 Program (No. 2013CB932604), NSF of China (Nos. 51535005 and 51472117), China Scholarship Council, and China Postdoctoral Science Foundation (No. 2016M600408).

[1] P. L. Llewellyn, S. Bourrelly, C. Serre, Y. Filinchuk, and G. Férey, Angew. Chem. **118**, 7915 (2006).
[2] K. L. Mulfort and J. T. Hupp, J. Am. Chem. Soc. **129**, 9604 (2007).
[3] J. Lee, O. K. Farha, J. Roberts, K. A. Scheidt, S. T. Nguyen, and J. T. Hupp, Chem. Soc. Rev. **38**, 1450 (2009).
[4] S. A. Hodgson, J. Adamson, S. J. Hunt, M. J. Cliffe, A. B. Cairns, A. L. Thompson, M. G. Tucker, N. P. Funnell, and A. L. Goodwin, Chem. Commun. **50**, 5264 (2014).
[5] G. Férey and C. Serre, Chem. Soc. Rev. **38**, 1380 (2009).
[6] A. B. Cairns, J. Catafesta, C. Levelut, J. Rouquette, A. Van Der Lee, L. Peters, A. L. Thompson, V. Dmitriev, J. Haines, and A. L. Goodwin, Nat. Mater. **12**, 212 (2013).
[7] A. B. Cairns and A. L. Goodwin, Phys. Chem. Chem. Phys. **17**, 20449 (2015).
[8] A. L. Goodwin, M. Calleja, M. J. Conterio, M. T. Dove, J. S. Evans, D. A. Keen, L. Peters, and M. G. Tucker, Science **319**, 794 (2008).
[9] T. D. Bennett, A. L. Goodwin, M. T. Dove, D. A. Keen, M. G. Tucker, E. R. Barney, A. K. Soper, E. G. Bithell, J.-C. Tan, and A. K. Cheetham, Phys. Rev. Lett. **104**, 115503 (2010).
[10] J.-C. Tan, B. Civalleri, C.-C. Lin, L. Valenzano, R. Galvelis, P.-F. Chen, T. D. Bennett, C. Mellot-Draznieks, C. M. Zicovich-Wilson, and A. K. Cheetham, Phys. Rev. Lett. **108**, 095502 (2012).
[11] A. U. Ortiz, A. Boutin, A. H. Fuchs, and F.-X. Coudert, Phys. Rev. Lett. **109**, 195502 (2012).
[12] M. Calleja, A. L. Goodwin, and M. T. Dove, J. Phys.: Condens. Matter **20**, 255226 (2008).
[13] A. M. Walker, B. Civalleri, B. Slater, C. Mellot-Draznieks, F. Corà, C. M. Zicovich-Wilson, G. Román-Pérez, J. M. Soler, and J. D. Gale, Angew. Chem., Int. Ed. **49**, 7501 (2010).
[14] A. L. Goodwin, D. A. Keen, and M. G. Tucker, Proc. Natl. Acad. Sci. U. S. A. **105**, 18708 (2008).
[15] H. Fang, M. T. Dove, and K. Refson, Phys. Rev. B **90**, 054302 (2014).
[16] S. Grimme, J. Antony, S. Ehrlich, and H. Krieg, J. Chem. Phys. **132**, 154104 (2010).
[17] A. Tkatchenko and M. Scheffler, Phys. Rev. Lett. **102**, 073005 (2009).
[18] M. Dion, H. Rydberg, E. Schröder, D. C. Langreth, and B. I. Lundqvist, Phys. Rev. Lett. **92**, 246401 (2004).
[19] V. Blum, R. Gehrke, F. Hanke, P. Havu, V. Havu, X. Ren, K. Reuter, and M. Scheffler, Comput. Phys. Commun. **180**, 2175 (2009).
[20] J. P. Perdew, K. Burke, and M. Ernzerhof, Phys. Rev. Lett. **77**, 3865 (1996).
[21] A. Tkatchenko, R. A. DiStasio, Jr., R. Car, and M. Scheffler, Phys. Rev. Lett. **108**, 236402 (2012).
[22] A. Ambrosetti, A. M. Reilly, R. A. DiStasio, Jr., and A. Tkatchenko, J. Chem. Phys. **140**, 18A508 (2014).
[23] Y. Zhang and W. Yang, Phys. Rev. Lett. **80**, 890 (1998).
[24] J. Klimeš, D. R. Bowler, and A. Michaelides, J. Phys.: Condens. Matter **22**, 022201 (2010).
[25] A. Togo, F. Oba, and I. Tanaka, Phys. Rev. B **78**, 134106 (2008).
[26] G. Kresse and J. Furthmüller, Phys. Rev. B **54**, 169 (1996).
[27] T. Bučko, S. Lebègue, J. G. Ángyán, and J. Hafner, J. Chem. Phys. **141**, 034114 (2014).
[28] P. Hermet, J. Catafesta, J.-L. Bantignies, C. Levelut, D. Maurin, A. Cairns, A. Goodwin, and J. Haines, J. Phys. Chem. C **117**, 12848 (2013).
[29] A. M. Reilly and A. Tkatchenko, J. Chem. Phys. **139**, 024705 (2013).
[30] J. G. Brandenburg and S. Grimme, Top. Curr. Chem. **345**, 1 (2014).
[31] D. A. Keen, M. T. Dove, J. S. Evans, A. L. Goodwin, L. Peters, and M. G. Tucker, J. Phys.: Condens. Matter **22**, 404202 (2010).
[32] N. Ferri, R. A. DiStasio, Jr., A. Ambrosetti, R. Car, and A. Tkatchenko, Phys. Rev. Lett. **114**, 176802 (2015).
[33] A. L. Goodwin, private communication (2016).
[34] A. Tkatchenko, A. Ambrosetti, and R. A. DiStasio, Jr., J. Chem. Phys. **138**, 074106 (2013).
[35] R. A. DiStasio, Jr., O. A. von Lilienfeld, and A. Tkatchenko, Proc. Natl. Acad. Sci. U. S. A. **109**, 14791 (2012).
[36] V. V. Gobre and A. Tkatchenko, Nat. Commun. **4**, 2341 (2013).
[37] N. Marom, R. A. DiStasio, Jr., V. Atalla, S. Levchenko, A. M. Reilly, J. R. Chelikowsky, L. Leiserowitz, and A. Tkatchenko, Angew. Chem., Int. Ed. **52**, 6629 (2013).
[38] A. L. Goodwin, D. A. Keen, M. G. Tucker, M. T. Dove, L. Peters, and J. S. Evans, J. Am. Chem. Soc. **130**, 9660 (2008).